

LIMITING FACTORS IN THE PERFORMANCE OF RAIL GUNS

O. Fitch* & M. F. Rose
Naval Surface Weapons Center
Dahlgren, Virginia

Summary

This paper examines the theoretical limits to the efficiency of a rail gun. The distinguishing feature of all rail guns is the need to have solid monolithic conductors for the rails. These rails impose an ultimate limit to the efficiency possible due to skin depth constrained electrical resistance. This paper examines the theory required to evaluate such effects and explores several possible rail gun configurations which allow an increase in ultimate efficiency. The design and construction of an experimental test bed is described as well as the operation of a novel crowbar switch which operates in microseconds and crowbars an inductor at a voltage zero.

Introduction

The most common means of accelerating masses to high velocities is to use chemical explosives or propellants. These methods have inherent limitations which make it difficult to obtain velocities greater than 2 km/sec. Because of this, there has been a long standing interest in the use of electrical energy to propel masses. Since these techniques involve electromagnetic forces, hypervelocities (10 km/sec) should be readily achievable with substantial masses. These concepts were actively investigated by the Germans⁽¹⁾ in WW II and have been studied more or less continuously ever since.

Recent advances in pulse power technology⁽²⁾ as well as milestone experiments by Marshall and Barber⁽³⁾ have resulted in major programs in DARPA and the U.S. Army to assess feasibility, practicality and utility of these devices as advanced weapons. Further, DOE and NASA⁽⁴⁾ have interests in using electromagnetic mass drivers for inertial confinement fusion and space launching.

One of the primary concepts being evaluated is the rail gun which consists of parallel conducting rails, energized by a pulsed source and shunted by a projectile which is free to move under the influence of the resulting magnetic forces. This technique is deceptively simple. Complex and subtle phenomena limit its ultimate utility. In this paper, we describe theoretically some of the limitations to this technique along with the design and construction of a simple test bed which is to be used to verify predicted performance from the theoretical models.

Theoretical

The energy efficiency of any mass driver is given by the formula:

$$\epsilon = \frac{E_K}{E_K + E_L} = \frac{1}{1 + \frac{E_R}{E_K} + \frac{E_S}{E_K}} \quad (1)$$

*Current Address
Training Air Wing Four
NAS, Corpus Cristi, TX 78419

where E_K and E_L are the kinetic energy delivered to the projectile and the energy lost in the process respectively. Further, for our purposes, $E_L = E_R + E_S$, where E_R is the energy dissipated in the ohmic resistance of the system and E_S is the energy stored in the system inductances. Both the skin depth limited resistance and the inductively stored energy divided by the kinetic energy in the projectile at rail exit are unique functions of the output parameters of the gun and for a given design, will govern the maximum conversion efficiency possible.

Consider the idealized rail gun shown in Figure 1. An ideal time varying current source, lossless leads, two parallel monolithic rails of ohmic conductor of length L , and a very thin lossless conducting projectile/shunt comprise the single system to be analyzed. The rails have length L , height h , conductivity σ and inductance per unit length $\frac{dL}{dx}$. The projectile has mass m . The force on the projectile is:

$$F = \frac{1}{2} \frac{dL}{dx} I^2 \quad (2)$$

Integrating gives the velocity and position of the projectile as a function of time. For simplicity and general applicability, it is convenient to solve these equations using non dimensional parameters. Let $\tau = t/t_0$ and $J(\tau) = I/I_0$ where t is the time for the projectile at position of maximum length and I_0 is the peak current.

$$v(\tau) = v_0 + \frac{1}{2m} \frac{dL}{dx} I_0^2 t_0 \int \{I_1(\tau)\} \quad (3)$$

$$x(\tau) = v_0 t_0 \tau + \frac{1}{2m} \frac{dL}{dx} I_0^2 t_0^2 \int \{I_2(\tau)\} \quad (3a)$$

where the integrals $I_1(\tau)$ and $I_2(\tau)$ are $\int_0^\tau J^2(\tau) d\tau$ and $\int_0^\tau \int_0^\tau J^2(\tau) d\tau d\tau$.

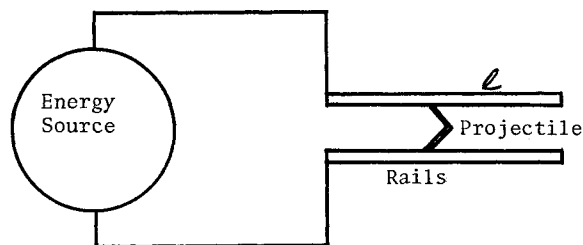


Figure 1. Rail Gun Schematic

Report Documentation Page				Form Approved OMB No. 0704-0188	
Public reporting burden for the collection of information is estimated to average 1 hour per response, including the time for reviewing instructions, searching existing data sources, gathering and maintaining the data needed, and completing and reviewing the collection of information. Send comments regarding this burden estimate or any other aspect of this collection of information, including suggestions for reducing this burden, to Washington Headquarters Services, Directorate for Information Operations and Reports, 1215 Jefferson Davis Highway, Suite 1204, Arlington VA 22202-4302. Respondents should be aware that notwithstanding any other provision of law, no person shall be subject to a penalty for failing to comply with a collection of information if it does not display a currently valid OMB control number.					
1. REPORT DATE JUN 1983		2. REPORT TYPE N/A		3. DATES COVERED -	
4. TITLE AND SUBTITLE Limiting Factors In The Performance Of Rail Guns				5a. CONTRACT NUMBER	
				5b. GRANT NUMBER	
				5c. PROGRAM ELEMENT NUMBER	
6. AUTHOR(S)				5d. PROJECT NUMBER	
				5e. TASK NUMBER	
				5f. WORK UNIT NUMBER	
7. PERFORMING ORGANIZATION NAME(S) AND ADDRESS(ES) Naval Surface Weapons Center Dahlgren, Virginia				8. PERFORMING ORGANIZATION REPORT NUMBER	
9. SPONSORING/MONITORING AGENCY NAME(S) AND ADDRESS(ES)				10. SPONSOR/MONITOR'S ACRONYM(S)	
				11. SPONSOR/MONITOR'S REPORT NUMBER(S)	
12. DISTRIBUTION/AVAILABILITY STATEMENT Approved for public release, distribution unlimited					
13. SUPPLEMENTARY NOTES See also ADM002371. 2013 IEEE Pulsed Power Conference, Digest of Technical Papers 1976-2013, and Abstracts of the 2013 IEEE International Conference on Plasma Science. Held in San Francisco, CA on 16-21 June 2013. U.S. Government or Federal Purpose Rights License					
14. ABSTRACT					
15. SUBJECT TERMS					
16. SECURITY CLASSIFICATION OF:			17. LIMITATION OF ABSTRACT SAR	18. NUMBER OF PAGES 5	19a. NAME OF RESPONSIBLE PERSON
a. REPORT unclassified	b. ABSTRACT unclassified	c. THIS PAGE unclassified			

Regardless of the rail thickness, magnetic diffusion causes the current to flow in a thin layer on the inside surface of the rails. The depth of this layer is a function of time and position and can be readily calculated. Neglecting fringing fields, each segment of rail, dx , sees a step function magnetic field applied at the moment the projectile passes. The penetration depth (δ) or "skin depth" at this segment is:

$$\delta = \sqrt{2(t - \theta)/\mu\sigma} \quad (4)$$

where θ is the time of projectile passage at the segment of interest, μ is the magnetic permeability and σ the conductivity of the rails. The differential resistance is then:

$$dR(t, x(t)) = \frac{dx}{\sigma h \delta} \quad (5)$$

for rails of height h .

Integrating gives

$$R(r) = \frac{2v_0}{h} \sqrt{\frac{\mu}{\sigma}} \sqrt{t_2/r} + \frac{1}{2mh} \frac{dL}{dx} \sqrt{\frac{\mu}{\sigma}} I_0^2 t_c^{3/2} \{I_3(r)\} \quad (6)$$

and $I_3(r)$ is nondimensional and given by $\int_0^r \left[\frac{\int_0^\tau J^2(\phi) d\phi}{1-r-\phi} \right] d\phi$.

The rail power dissipation is then

$$E_r = \sqrt{\frac{2\mu}{\sigma}} \left[\frac{2v_0}{h} (t_2)^{3/2} I_0^2 \{I_4(r)\} + \frac{1}{2mh} \frac{dL}{dx} I_0^4 t_c^{5/2} \{I_5(r)\} \right] \quad (7)$$

$$\text{where } I_4 = \int_0^r \sqrt{1-r-\tau} J^2(\tau) d\tau$$

$$I_5 = \int_0^r J^2(\tau) \left[\int_0^\tau \left(\frac{\int_0^\phi J^2(\phi) d\phi}{1-r-\phi} \right) d\phi \right] d\tau$$

In a similar fashion, we can derive an expression for E_k :

$$E_k = \frac{1}{2} \frac{dL}{dx} I_0^2 t_c v_0 \{I_1(r)\} + \frac{1}{4m} \left(\frac{dL}{dx} \right)^2 I_0^4 t_c^2 \{I_6(r)\} \quad (8)$$

$$\text{where } I_6(r) = \int_0^r J^2(\tau) \left[\int_0^\tau J^2(\tau) d\tau \right] d\tau$$

E_k refers solely to the electrically derived kinetic energy in the projectile. To find the total projectile kinetic energy, one must add $1/2 mv_0^2$ from whatever injection scheme was used. After algebraic manipulation,

$$\frac{E_r}{E_k} = \frac{2\sqrt{2}}{h \frac{dL}{dx}} \sqrt{\frac{\mu}{\sigma}} \sqrt{t_c} \left\{ \frac{2v_0 I_4 + \frac{1}{2m} \frac{dL}{dx} I_0^2 t_c I_5}{v_0 I_1 + \frac{1}{2m} \frac{dL}{dx} I_0^2 t_c I_6} \right\} \quad (9)$$

The dependence on the expulsion time t_c , while interesting, is not unique to the design of a gun. Noting that $v = v_f$ and $x = \ell$ at exit,

$$t_c = \left(\frac{I_1}{I_2} \right) \left[\frac{1}{1 + \left(\frac{I_1}{I_2} - 1 \right) \frac{v_0}{v_f}} \right] \left(\frac{\ell}{v_f} \right) \quad (10)$$

and

$$\frac{1}{2m} \frac{dL}{dx} I_0^2 = \frac{v_f - v_0}{t_c I_1} \quad (11)$$

substituting gives the value of $\frac{E_r}{E_k}$ at muzzle exit.

$$\frac{E_r}{E_k} = A \left(\frac{1}{h \frac{dL}{dx}} \right) \sqrt{\frac{\mu}{\sigma}} \sqrt{\frac{\ell}{v_f}} \quad (12)$$

where A is a dimensionless number of order 1 and given by

$$A = 2\sqrt{2} \sqrt{\frac{I_1}{I_2}} \left(\frac{I_5}{I_6} \right) \left\{ \frac{1 + 2 \left(\frac{I_4 I_1}{I_5} - 1 \right) \frac{v_0}{v_f}}{1 + \left(\frac{I_1}{I_2} - 1 \right) \frac{v_0}{v_f}} \right\} \frac{1}{1 + \left(\frac{I_1}{I_2} - 1 \right) \frac{v_0}{v_f}}$$

where Υ has also been set to 1.

Similarly, we may show that:

$$\frac{E_s}{E_k} = J^2(r) \left(\frac{I_2(r)}{I_6(r)} \right) \left[\frac{1 + \left(\frac{I_1(r)}{I_2(r)} - 1 \right) \frac{v_0}{v_f}}{1 + \left(\frac{I_1(r)}{I_2(r)} - 1 \right) \frac{v_0}{v_f}} \right] \quad (13)$$

which is zero if the current is zero when the projectile leaves the rail system.

Equations 12 and 13 allow interesting insight into the factors governing rail gun performance. First, in our formulation, E_r/E_k is dependent on a dimensionless parameter (A) which is purely a function of the shape of the current profile, injection velocity v_0 and the final velocity v_f the gun is designed to achieve. This number should be minimized for maximum efficiency. The rail height and inductance/unit length should be made as large as possible, but since h is coupled to dL/dx through the formula for L , increasing h usually decreases dL/dx . However, some improvements can be made by increasing h . The material parameters μ & σ are pretty much fixed for a given material. However, cryogenic operation does give some improvement in E_r/E_k by increasing σ . Finally a shorter barrel length is desirable, but that in turn, necessitates higher currents to achieve a given v_f . The ratio E_r/E_k is absolutely minimized by letting I drop to zero as the projectile exits the barrel. While that is desirable, it is not always practical.

As an example, let us consider the applications of the above to a 20mm square bore rail gun, using copper rails but energized with three wave shapes corresponding to $J^2(r) = 1, \Upsilon, 1-\Upsilon$. Table 1

illustrates the theoretically predicted performance when E_s is assumed to be recoverable.

Table 1.
CURRENT PROFILE EFFICIENCIES

Current Profile	*	**	***
	A	E_r/E_k	ϵ
$J^2(\tau) = 1$	4.27	1.28	43.9% (30%)
$J^2(\tau) = \tau$	4.64	1.39	41.8% (29%)
$J^2(\tau) = 1 - \tau$	3.28	.98	50.5%

* = $v_o/v_f = 0$

** = $h = 20\text{mm}$, $\frac{dL}{dx} = 0.628 \frac{\mu\text{H}}{\text{m}}$, $L = 2\text{m}$, $v_f = 3 \text{ km/sec}$

*** = The numbers in parenthesis are efficiencies assuming the energy stored in the rail system is not recovered.

Clearly the current profile which reduces the energy stored in the rails to 0 is the most efficient design. This is accomplished by reducing skin depth losses as well as energy stored in the rail inductance. The disadvantage however is that the peak pressure in the rails is much greater than for the other profiles considered and, in fact, may lead to a nonrealizable design because of material constraints.

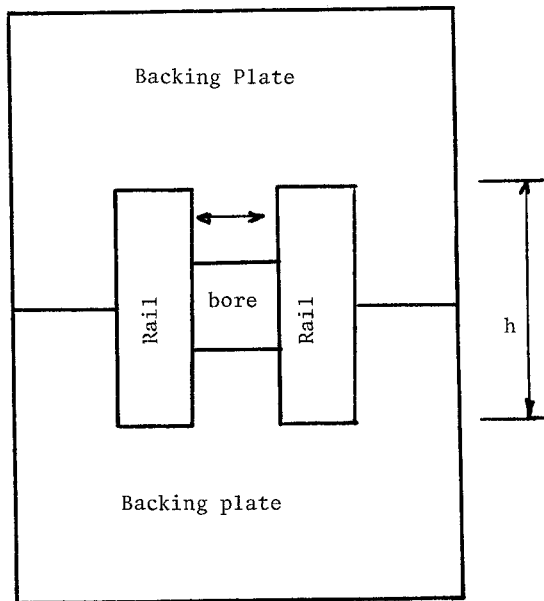


Figure 2. Rail Configuration Increasing h

The skin depth limited efficiency of the gun can be improved by increasing the product $h \frac{dL}{dx}$. Figure 2 shows a design where the rail width h has been allowed to extend beyond the edges of the bore. This configuration increases $h \frac{dL}{dx}$ substantially but does so at the expense of a decrease in $\frac{dL}{dx}$. Table 2 illustrates possible gains with this configuration.

Table 2.
EFFECT OF SKIN DEPTH AND h
ON GUN EFFICIENCY FOR OHMIC LOSSES ONLY

h/s	dL/dx	$h dL/dx^*$	E_r/E_k^{**}	ϵ^{***}
0.1	1.5214	3.04×10^{-3}	5.29	15.9%
0.5	0.8852	8.85×10^{-3}	1.82	35.5%
1.0	0.6283	1.26×10^{-2}	1.28	43.9%
2.0	0.4070	1.63×10^{-2}	1.01	49.7%
3	0.3058	1.83×10^{-2}	0.88	53.3%
10	0.1104	2.21×10^{-2}	0.72	57.7%
100	0.01257	2.51×10^{-2}	0.64	61.0%
	0	2.51×10^{-2}	0.64	61.0%

* = Assumes $S = 20\text{mm}$

** = $\frac{1}{2} \frac{v_o^2}{v_f^2}$, $v_f = 3 \text{ km/sec}$, $L = 2\text{m}$, $A = 64/15$

*** = Assumes all inductively stored energy is recoverable.

The effect of changing $h \frac{dL}{dx}$ for the case considered (constant current) makes it necessary to raise I_o if the same exit velocity is to be achieved. A simple calculation shows that:

$$I_{RB} = I_{SB} \sqrt{\left(\frac{dL}{dx}\right)_{SB} / \left(\frac{dL}{dx}\right)_{RB}} \quad (14)$$

where the subscripts RB and SB refer to rectangular bore and square bore respectively.

A pictorial representation of the current streamlines is shown in Figure 3.

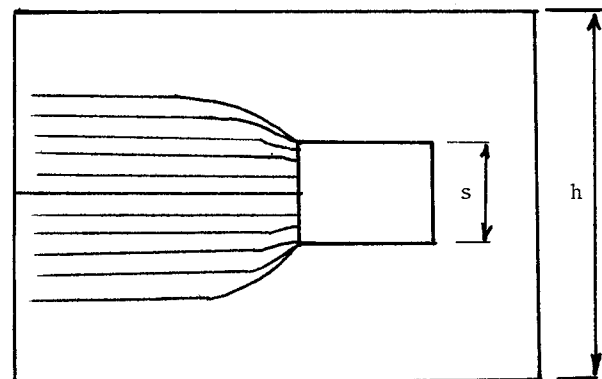


Figure 3. Current streamlines for Rectangular bore

Since all the current must flow through the projectile, the maximum stress sustained by the rail system is at the position of the projectile and is exactly the same as that for a square bore system carrying the same current. The stress in a

rectangular bore gun is everywhere lower than that for a square bore gun except at the position of the projectile, where the stresses are equal. Also, the total force on the rails of a rectangular bore gun is equal to that of a square bore gun. The only disadvantage to a rectangular bore gun is that higher currents are required which translates into additional power supply requirements.

As an example, from the data in tables 1 and 2, we compare the efficiency obtainable for a square bore, constant current gun with that of a rectangular bore ($h/s = 3$) and decaying current pulse ($J^2 = 1 - \tau$). Both have 20mm projectiles and it is assumed that residual energy stored in system inductances is not recoverable. Table 3 illustrates the calculation.

Table 3.
Gun Comparison

	A	$h \frac{dL}{dx}$	E_r/E_k	E_r/E_k	ξ^*
"Improved Gun"	3.28	1.8×10^{-2}	0.67	0	60%
Base Design Gun	4.27	1.3×10^{-2}	1.28	1	30.5%

* $v_f = 3$ km/sec, $\ell = 2$ m, copper rails

The figures in table 3 clearly indicate that improvements in efficiency can be had by judicious choice of gun parameters. These calculations are however intended only to show trends. Detailed gun design must take into account armature design and losses, bursting stresses for the rails and the details of the power supply. It is worth noting that although these calculations are only an approximate guide to real gun efficiencies, they are valuable in that they indicate the amount of waste energy (heat) which must be removed from the system.

Experimental

In order to test some of the concepts discussed above, a small rail gun facility was constructed which is initially driven by a 20 kJ 20 kV capacitor bank. We were especially interested in a drooping current profile. Hence, the capacitance stored energy is first stored in an inductor and trapped by means of a crowbar switch. The trapped flux is then allowed to expand against the projectile/armature doing work as the projectile is accelerated down the bore. The gun is shown schematically in Figure 4.

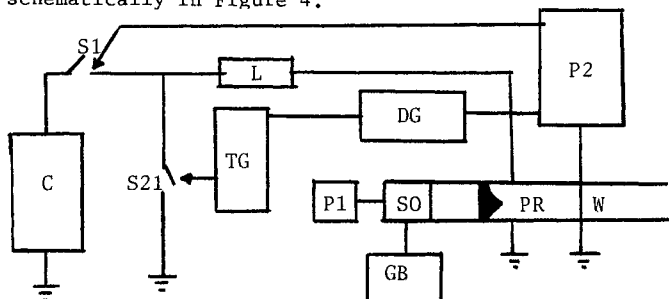


Figure 4. Gun Schematic

The sequence of operation is as follows: The gas bottle (GB) is charged to a pressure (P). The solenoid valve (SO) is energized from the pulser (P1), driving the projectile (PR) down the rail

system with a velocity v_0 . The projectile breaks the wire (W) sending a pulse to fire the capacitor bank (C) at switch S_1 . Simultaneously, the delay generator (DG) begins counting and sends a signal to the trigger generator (TG) after a time t which is picked to correspond to the condition ($V = 0$, $I = I_{max}$). At that time, the crowbar switch (S_2) is fired, trapping flux in the storage inductor L and the rail system. Under the influence of the magnetic pressure and the residual gas pressure, the projectile accelerates down the rail system. The basic parameters of the gun as configured are: $\ell = .92$ m, $\frac{dL}{dx} = 0.32 \mu\text{H/m}$, $h = 2.5$ cm and $s = 1.25$ cm. The inductor as originally configured is one turn of 4-0 welding cable with an inductance of $0.95 \mu\text{H}$ and a resistance of $1.0 \text{ m}\Omega$. Our 14 gram projectile was accelerated to 70 m/sec. The inductor is charged to 200 kA in $15 \mu\text{s}$.

The crowbar switch must meet the following requirements: (1) It must hold off an initial voltage of 20 kV (2) Must positively close near a voltage zero and (3) Pass currents in excess of 200 kA. Further, it must be triggerable with jitter less than $1 \mu\text{s}$. The basic switch is shown in Figure 5.

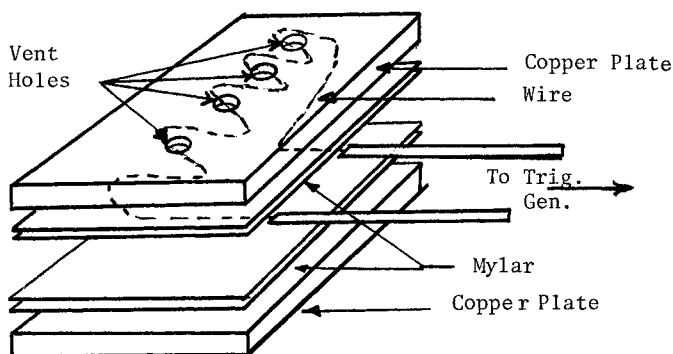


Figure 5. Drawing of Switch

In its simplest form, two flat copper plates/electrodes are separated by layers of mylar sufficient to hold off the maximum voltage of the system. Layered within the mylar is an exploding wire, powered by a small fast bank. When the crowbar bank is fired, a high current pulse causes the wire to explode on the microsecond time scale, driving the mylar into the copper plates. Here the mylar encounters a regular series of holes or sharp edge depressions which shear the mylar. Since the mylar is only a few mils thick, the resultant shear area is filled with hot metal plasma from the exploding wire which provides a positive closure and an excellent current conduction path for current from the inductor.

In practice, the whole assembly is bolted together to keep the plates from separating due to the dynamic forces produced by the exploding wire and the subsequent current pulse as the inductor discharges. The exploding wires used by us were 0.010" aluminum and were exploded using the output from a triggered 40 kV, $0.44 \mu\text{F}$ capacitor bank. The switch performed reliably with only minor degradation of performance as the plates became worn. The peak currents carried were greater than 100 kA and hold off voltages in excess of 10 kV. Maximum conduction time for this switch was on the order of 1 ms.

Figure 6 shows an experimental trace showing a complete firing of the gun at the 10 kv level. Both traces shows the current-time profile in the inductor as measured by a Rogowski probe.

Initially the current follows a typical LC sine wave and it is during this time that the switch must hold off the maximum voltage. Trace 1 is $5 \mu\text{s/cm}$ and measures a peak current of 100 kA. Trace 2 is $50 \mu\text{s/cm}$ and shows the L/R decay typical of the storage inductance discharging into the switch impedance. By measuring the time constant, the switch impedance was $\sim 1 \text{ m}\Omega$, which gives a voltage drop across the switch of some 70 volts. Further experimentation with this gun awaits the construction of our 250 kJ capacitor bank.

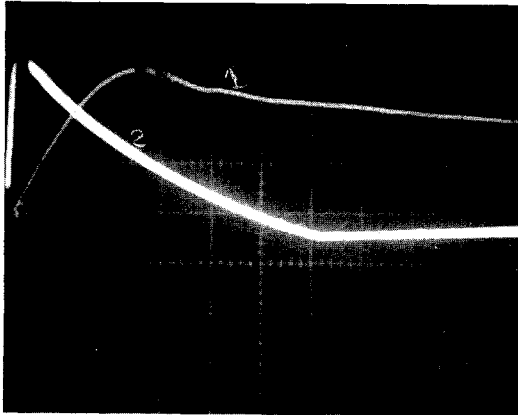


Figure 6. Scope trace showing current-time profile for experimental assembly

Discussion

This simple theory as we have derived it should not be construed as accurate in an absolute sense. It should however be quite adequate to assess trends and to do a comparative analysis of competing gun designs, noting that all real gun efficiencies will be less than those predicted by the theory.

Clearly $h \frac{dL}{dx}$ is an extremely important parameter in the design of a system. The optimum value however may not be realizable because of material constraints. Second in importance is the shape of the current pulse. The rail configuration is not easily amenable to energy recovery from the system at projectile exit, therefore some combination of constant current ($J^2 = 1$) and current drop off ($J^2 = 1 - \gamma$) is probably an optimum solution which would minimize the rail length L for a given velocity v_f . This implies pulse shaping which will greatly influence the design of the pulse power train. Finally, the parameter μ/σ can be controlled somewhat by cryogenic cooling. It is easy to show that this effect at liquid nitrogen temperature) can improve the efficiency by some 7-10%.

The same temperature effect however will degrade system performance as the heat builds up in the system. At 500°C , the system performance will be degraded by some 10%. Clearly wild swings in system impedance is undesirable and will place severe requirements on the pulse power train or necessitate an adequate cooling system if high repetition rate is desired.

References

This work is supported by the Independent Exploratory Development Program at the Naval Surface Weapons Center.

1. "Electric Gun and Power Source," Armour Research

Foundation, AD499 966.

2. "Proceedings of the 3rd IEEE Pulsed Power Conference," IEEE Catalog 81CH1662-6, 1981.

3. J. P. Barber, "The Acceleration of Macroparticles and a Hypervelocity Electromagnetic Accelerator," Ph.D. Thesis, Australian National University, Canberra, 1972.

4. "Conference on Electromagnetic Gun and Launchers," DARPA/ARRADCOM, San Diego, Nov. 1980.